Real-Time FPGA-Based Multi-Beam Directional Sensing of 2.4 GHz ISM RF Sources

Sravan Pulipati*, Viduneth Ariyarathna*, Chamira U. S. Edussooriya†, Chamith Wijenayake‡, Xin Wang§ and Arjuna Madanayake*
*Department of Electrical and Computer Engineering, Florida International University, Miami, FL, USA
†Department of Electronic and Telecommunication Engineering, University of Moratuwa, Moratuwa, Sri Lanka
‡School of Electrical Engineering and Telecommunications, University of New South Wales, Sydney, NSW, Australia
§Department of Electrical and Computer Engineering, Stony Brook University, Stony Brook, NY, USA
Emails: {spuli009, pberu002, amadanay}@fiu.edu, chamira@ent.mrt.ac.lk,
c.wijenayake@unsw.edu.au, x.wang@stonybrook.edu

***Abstract*—A real-time directional sensing system is proposed for 2.4 GHz ISM band by exploiting the concept of spatio-temporal spectral white spaces. The proposed system consists of a 16-element patch antenna array, an FFT-based multi-beam beamformer and an energy detector. Our system operates at the baseband with quadrature sampling. Furthermore, digital architectures for two energy detectors that employ integrate-and-dump circuits are presented. With the multi-beam beamformer, the first energy detector can be employed to directional sensing and the second can be employed for both directional and spectral sensing of radio frequency sources. The multi-beam beamformer having 16 beams and the energy detectors are implemented on a ROACH-2 based FPGA system with a 160 MHz clock. With an 8-point temporal FFT, the second energy detector provides approximately 20 MHz bandwidth per temporal FFT-bin. Preliminary experimental measurements obtained with Wi-Fi devices and the first energy detector verify the proof-of-concept directional sensing of the proposed system.**

***Index Terms*—Cognitive radio, directional sensing, spectrum sensing, white space, FPGA, multi-beam beamforming.**

I. Introduction

The exponential growth of wireless systems and networks is leading to scarcity of available radio spectrum [1]–[3]. Wireless frequency channels are being increasingly occupied. However, the spatio-temporal nature of wave propagation and underlying spectral sparsity has rarely been exploited for frequency reuse. This lack of sharing of carrier frequency as a function of propagation direction occurs despite the fact that the wireless channels appear extremely sparse in a spatio-temporal frequency domain [4]. Spatio-temporal sparsity makes such channels ripe for directional channel multiplexing for increased system capacity. In [5], the multi-dimensional Fourier transform of propagating electromagnetic plane waves, which are the far-field solutions to the wave-equation that models wireless channels, was shown to possess a region of support (ROS) in the spatio-temporal Fourier (i.e., frequency) domain that is 1) enclosed in the region of causality (light cone) [6, ch. 6], and 2) constrained to be on line-shaped segments that are aligned in orientation to the direction of propagation of the plane waves in free space [5]. In this paper, we propose a radio frequency (RF) multi-beam array receiver for the sensing of RF sources operating in the 2.4 GHz ISM band, such as Wi-Fi devices, taking into account both channel frequency and direction of propagation. The proposed system operates at the baseband (i.e., with down-converted and quadrature sampled in-phase (I) and quadrature-phase (Q) signals), and a fast Fourier transform (FFT)-based multi-beam beamformer implemented on ROACH-2 field-programmable gate array (FPGA) system is employed for real-time directional sensing. Experimental measurements obtained using Wi-Fi devices are presented to verify the proof-of-concept directional sensing of the proposed system.

978-1-7281-3632-5/19/$31.00 ©2019 IEEE

II. Related Work in Spectrum Sensing

Cognitive radio networks attempt to alleviate spectral scarcity by exploiting opportunistic communication channels, identified via a spectrum sensing and monitoring subsystem within an overall dynamic spectrum management and allocation system. Such spectrum sensing and monitoring techniques have been continuously explored since the early days of cognitive radio [1], [2], [7] and a fairly recent and comprehensive survey can be found in [3], [8] and references therein. Formulation of *spectral holes* or *spectral white spaces* is typically done considering spectral usage characteristics over multiple dimensions such as time, frequency, direction, location, and code; for example, the concept of 4-D spectral holes and cooperative beamforming based spectrum sensing were presented in [9]. For narrowband spectrum sensing, low-complexity non-coherent energy detection is commonly used, while more computationally intensive matched filter-based techniques, (cyclostationary) feature detectors, and eigenvalue-based detectors are used when coherent detection is required [3]. Several wideband techniques are also reviewed in [3] including both critically sampled and sub-Nyquist sensing techniques. In [10], polarization of the electromagnetic waves has been exploited to sense the presence of a primary user signal.

Opportunistic spectral access via spatial domain sparsity (hence spatial reuse of the available spectrum) has been explored in [11]–[20]. Such approaches typically exploit directional transmission and reception using directional sector antennas [16], [19], [21], beam steering via passive radiators with a single active element and a single RF chain [14], [15] and electronically scanned beamforming arrays [13], [17], [18]. In particular, [20] introduces the concept of spatial spectral holes and used relay assisted directional transmission to exploit spatial domain spectral sparsity via cooperative sensing.

Spectral occupancy measurement in an outdoor 5 GHz Wi-Fi network using directional antennas was demonstrated in [22] with a practical implementation and measurements. In [23], authors demonstrated a low-latency FPGA implementation of an energy detection based wideband spectrum sensor from 70 MHz to 6 GHz. The concept of spatio-temporal white spaces from a multidimensional signal processing perspective was presented in [4], [24] for direct converted RF signals and such directional sensing employing low-complexity array processing combined with cyclostationary feature detection was presented in [25]. In this paper, we present the directional spectrum sensing at the *baseband* using multidimensional signal processing perspective. Our approach is more efficient compared to the directional spectrum sensing presented in [4], [24] because of the significantly lower temporal sampling and the use of spatially-bandpass filters implemented using FFT algorithms compared to the spatio-temporal bandpass filters employed in [4].

III. Two-Dimensional Signal Processing Model and Spectra of Plane Waves at the Baseband

A. 2-D Spatio-Temporal Spectrum of a Plane Wave Received by a Uniform Linear Array

The two-dimensional (2-D) spatio-temporal signal model and the spectrum of a plane wave received by a uniform linear array (ULA) are presented in this section. To this end, we consider the directional sensing of an electromagnetic wave emanating from an RF source, such as a Wi-Fi enabled device, located in the far field by a ULA as shown in Fig. 1(a). In this case, the electromagnetic wave, denoted as $w_{\rm C}(x, ct)$, can be modeled as a propagating plane wave in the 2-D continuous spatio-temporal domain $(x, ct) \in \mathbb{R}^2$ [26, ch. 1], [6, ch. 6]. Here, ct is the temporal domain scaled by c, the constant speed of propagation of electromagnetic waves, and $\theta \in (-90^\circ, 90^\circ)$ denotes the direction of arrival (DOA). Note that $w_{\rm C}(x, ct)$ can be considered as either a *narrowband* signal or a *broadband* signal depending on the fractional bandwidth. In general, signals having fractional bandwidths greater than 5% are considered to be broadband [27]. It is shown in [5] that the *ideal* continuous-domain spectrum $W_{\rm C}(\Omega_x, \Omega_{ct})$ of $w_{\rm C}(x, ct)$ lies on a straight line going through the origin of the 2-D continuous frequency domain $(\Omega_x, \Omega_{ct}) \in \mathbb{R}^2$. Note that Ω_x is the continuous-domain spatial frequency and Ω_{ct} is the continuous-domain temporal frequency scaled by $1/c$, i.e., $\Omega_{ct} = \Omega_t/c$. The ROS of the spectrum $W_{\rm C}(\Omega_x, \Omega_{ct})$ consists of two segments lying on the straight line as shown in Fig. 1(b). The length of the straight line segments is determined by the temporal bandwidth of a plane wave. The angle α between the ROS of $W_{\rm C}(\Omega_x, \Omega_{ct})$ and the Ω_{ct} axis is given by [5], [28]

$$\alpha = \tan^{-1}(\sin(\theta)). \tag{1}$$

Note that $\alpha \in (-45^\circ, 45^\circ)$ because $\theta \in (-90^\circ, 90^\circ)$.

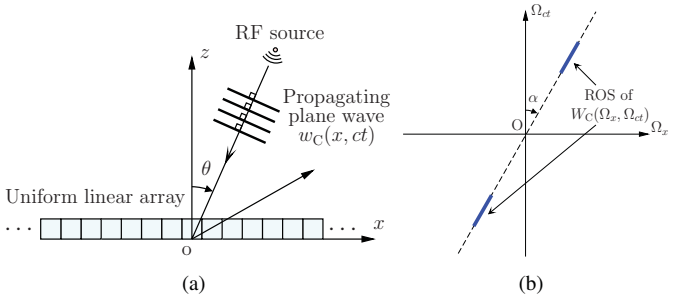

Fig. 1. (a) An RF signal received by a ULA; (b) The ROS of the spectrum of a plane wave signal in the 2-D frequency domain.

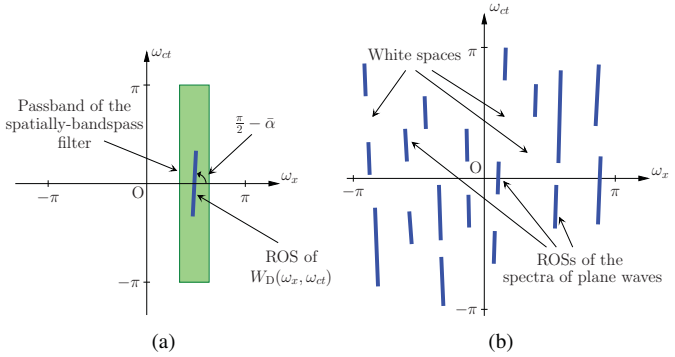

Fig. 2. (a) The ROS of the 2-D spectrum of a quadrature-sampled plane wave; (b) ROSs of the spectra of plane waves and white spaces.

B. 2-D Spatio-Temporal Spectrum at the Baseband

For an RF signal having a fractional bandwidth less than 50%, temporal sampling (i.e., analog-to-digital conversion) at the baseband is more economical than the temporal sampling at RFs. To this end, a plane wave is first processed through an RF front-end consisting of low-noise amplifiers and bandpass filters. Subsequently, the plane wave is down-converted to the baseband using local oscillators (LOs) and processed through lowpass filters for quadrature sampling with I and Q components [29, ch. 8], [30]. The quadrature-sampled 2-D discrete-domain signal $w_{\rm D}(n_x, n_{ct})$, $(n_x, n_{ct}) \in \mathbb{Z}^2$, is complex-valued. Furthermore, the ROS of the spectrum $W_{\rm D}(\omega_x, \omega_{ct})$, $(\omega_x, \omega_{ct}) \in \mathbb{R}^2$, of $w_{\rm D}(n_x, n_{ct})$ consists of a single line segment inside the principal Nyquist square $\mathcal{N}$ [31], [32] as shown in Fig. 2(a). This line segment is generated by down-shifting the upper segment of the ROS of $W_{\rm C}(\Omega_x, \Omega_{ct})$ (see Fig. 1(b)) [29, ch. 8], [30]. The principal Nyquist square is defined as $\mathcal{N} = \{(\omega_x, \omega_{ct}) \in \mathbb{R}^2, -\pi \leq \omega_x, \omega_{ct} < \pi\}$, and $\omega_i = \frac{2\pi\Omega_i}{\Omega_i^S}$ $(i = x, ct)$, where Ω_i^S is the corresponding sampling frequency. It is worthwhile to note that $w_{\rm D}(n_x, n_{ct})$ is predominantly a *broadband* signal at the baseband even though

$w_{\rm C}(x, ct)$ is narrowband at RFs. The angles $\bar{\alpha}$ corresponding to the ROS of $W_{\rm D}(\omega_x, \omega_{ct})$ can be derived as [31], [32]

$$\bar{\alpha} = \tan^{-1}\left(\frac{\Delta_x \tan(\alpha)}{\Delta_{ct}}\right), \tag{2}$$

where Δ_x and Δ_{ct} are the spatial and temporal sampling intervals, respectively. In our RF directional sensing system, the patch antennas are arranged with $\Delta_x = 0.06$ m (corresponding to a Nyquist frequency of 2.5 GHz) and the baseband temporal sampling frequency is selected 160 MHz leading to $\Delta_{ct} = 1.875$ m. Note that, with these specifications, $\bar{\alpha} \in (-1.83°, 1.83°)$ for $\theta \in (-90°, 90°)$ (or $\alpha \in (-45°, 45°)$). In this case, the ROS of $W_{\rm D}(\omega_x, \omega_{ct})$ is essentially parallel to the ω_{ct} axis. Consequently, such a plane wave can be sensed using a *spatially-bandpass* filter as shown in Fig. 2(a).

Let us consider the case where M (≥ 2) plane waves with different DOAs are received by the ULA. In this case, the ROSs of the spectra of quadrature-sampled plane waves consist of M single line segments inside the principal Nyquist square as shown in Fig. 2(b). The location of a straight line segment depends on the temporal bandwidth and the DOA of a plane wave. The presence of a plane wave or the absence of a plane wave (i.e., a white space) with respect to the DOA can be sensed using a multi-beam beamformer having spatially-bandpass responses as described in the next section.

IV. Sensing Over Multi-Beams

The 2-D spectrum of a discrete-domain plane wave is computed by using the 2-D discrete Fourier transform (DFT) using the FFT algorithms [33]. The 2-D DFT is a row-column separable operation. Therefore, we may compute the spatial FFT for each temporal sample, and then compute temporal FFTs along each of the spatial-FFT's column outputs, which appear as temporal sequences. The outputs of the spatial-FFT bins are in fact directional RF beams, with beam axis defined by the bin number of the spatial FFT. The N-point spatial-FFT can be computed using fixed-point arithmetic at arithmetic complexity $\mathcal{O}(N \log N)$ or approximated at low-complexity without using any multipliers at all, with about a 2 dB loss in directivity [34]. For directional sensing, we employ a multi-beam beamformer designed using spatial-FFT and realized on an FPGA. The beamformer produces 16 RF beams, which are in the mixed spatial-Fourier-temporal domains. These beams are used here for directional sensing using energy detectors presented in Sec.V, for real-time directional sensing of 2.4 GHz Wi-Fi sources. Fig. 3(a) shows the expected theoretical RF beams. Fig. 3(b) shows the measured beams from experimental evaluation using an anechoic chamber, with the FPGA operated at a clock frequency of 200 MHz.

V. Two-Dimensional Directional Sensing: Digital Architectures and Experimental Results

In this section, we present the 16-element RF receiver, the digital architectures for a multi-beam directional energy detector and a 2-D FFT-based spatio-temporal energy detector, and the experimental measurements obtained using Wi-Fi sources operating at the 2.4 GHz ISM band.

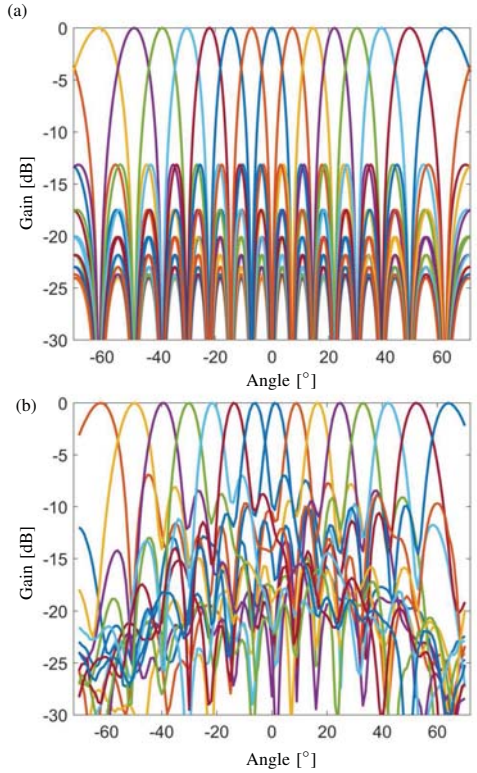

Fig. 3. (a) Theoretical RF beams corresponding to the spatial FFT outputs; (b) the experimentally measured beams using a fixed-point implementation of the 16-point FFT.

A. Antenna Array, RF Front-End and Digital Systems Setup

The overall system employed for experiments is shown in Fig. 4. The antenna array consists of 16 rectangular patch antennas opertaing at 2.4 GHz, and the RF front-end employs a 16-element single-mixer super-heterodyne architecture. The RF front-end is implemented using commercial-off-the-shelf components from www.minicircuits.com (combiner - *ZN2PD 63S+*, bandpass filter - *VBFZ 2340S+*, low-noise amplifier - *ZX60-242LN*, mixer - *ZFM-15S+*, lowpass filter -*SLF-550+*, intermediate frequency amplifier - *ZFL-1000LN+*). The LO signals are distributed to the 32 identical mixers using a microwave 1:16 splitter. Each of the outputs of the LO distribution system is split to 0°-90° for the I-Q direct-conversion mixers using hybrids. It is essential that all the RF signal generators are synchronized to the same reference clock to avoid frequency drifts. In our case, a 10 MHz reference from the NOISE XT ultra-low jitter signal generator is used to drive the VALON at receiver side for clocking ROACH-2 analog-to-digital converters (ADCs). NOISE XT generates frequencies from 2 MHz to 7 GHz with a resolution of 1 Hz and ultra-low noise floor down to -178 dBc/Hz. The VALON is a dual frequency synthesizer module whose frequency range spans from 23 MHz to 6 GHz, and provides 32 dB of attenuation control. The multi-beam beamformer is implemented on the ROACH-2 based FPGA system. Note that the ROACH-2 based FPGA system is a standard high-performance FPGA signal processing platform used in the radio astronomy community [35]. Our receiver provides a gain of 40 dB and have a

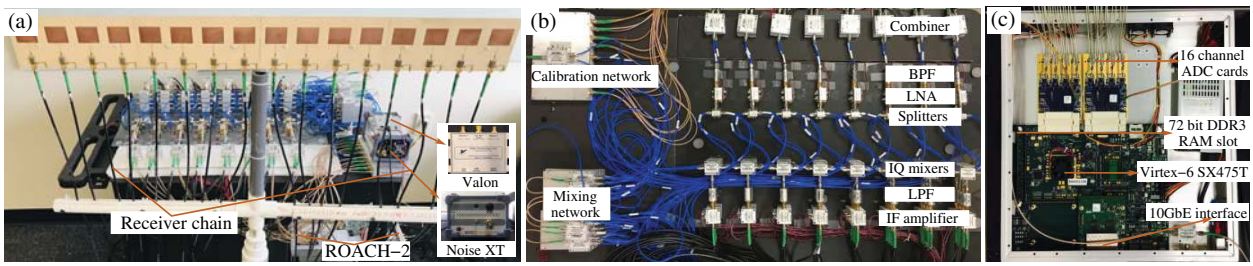

Fig. 4. (a) The overall experimental setup; (b) RF receiver chain implemented using commercial-off-the-shelf components; (c) ROACH-2 based FPGA system

noise figure of 4 dB. The reader is referred to our recent work [34] for more details of the antenna array, RF front-end and ROACH-2 based FPGA system.

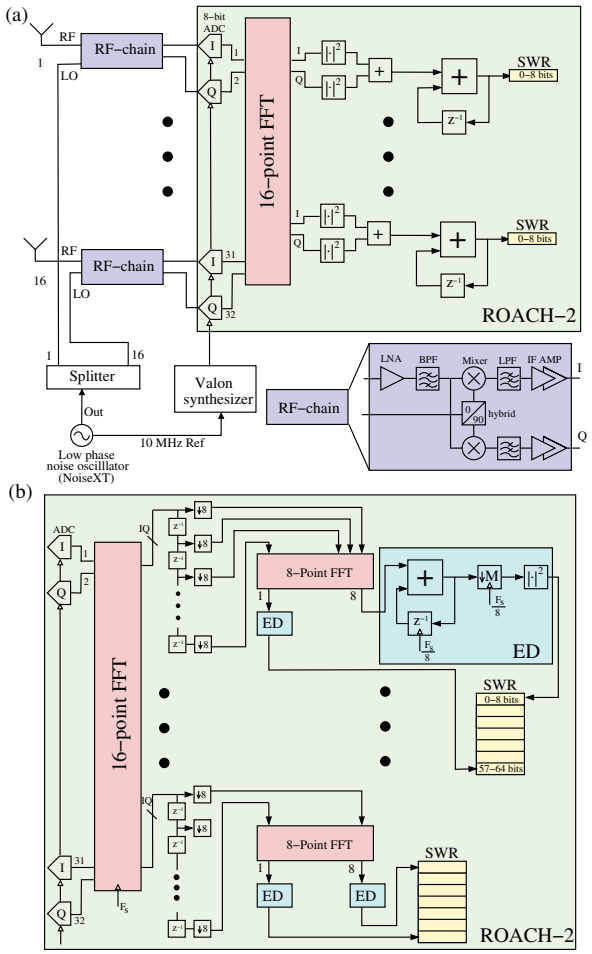

Fig. 5. Digital architectures for directional sensing of RF sources; (a) multi-beam directional energy detector; (b) average 2-D FFT-based PSD function.

B. Multi-Beam Directional Energy Detectors

Fig. 5(a) shows the full system implementation of the multi-beam directional energy detectors. Here, each of the parallel multi-beam RF signals are squared, integrated, and down-sampled (standard integrate-and-dump algorithm) for measuring the receive signal power at 16 simultaneous look directions using the FFT-based multi-beam beamformer described in Sec. IV. This is a simple energy detector where the signal content and features are not considered. The only measurands are DOAs and average received energy per beam (using a sliding-window approach). This energy detector allows the directional sensing but can not differentiate sources based on frequency, modulation type, bandwidth, or other features of the plane waves received. In this paper, we provide real-time experimental results for such "crude" RF sensing of Wi-Fi devices, operating in the 2.4 GHz ISM band, using our RF multi-beam receiver.

C. Average 2-D FFT-based Power Spectral Density Function

Fig. 5(b) shows ongoing extension to the architecture presented in the previous subsection, where we employ temporal DFTs for each of the beams obtained from the spatial-DFT based multi-beam beamformer. In fact, we compute the 2-D DFT of the antenna array output signal with respect to both discrete spatial and temporal dimensions, i.e., power spectral density (PSD) function. The architecture therefore requires one spatial-FFT core for the 16 beams, and 16 more temporal FFT cores for computing the temporal DFTs. Therefore, the digital circuit area is $\times 17$ larger than that of the previous architecture, based on the FFT-core area alone. In practice, the digital complexity is even larger due to bit-growth of the system word size as the signal progresses from the 32-ADC ports and through the different FFT stages. The 2-D FFT output bins correspond to an 16×8 matrix, assuming a basic 8-point temporal FFT per beam. The clock frequency of 160 MHz is chosen for the design so that each of the temporal FFT bin approximately covers a 20 MHz channel of the 2.4 GHz ISM band. The 2-D FFTs are integrated in a traditional integrate-and-dump loop to improve the signal to noise ratio (SNR) under the assumption of a quasi-static condition for the incident RF plane waves. The integration of K samples of each of the 2-D FFT bins leads to improve the SNR in the order of $\sqrt{K}$ because the signal is correlated and wide sense stationary additive white Gaussian noise is uncorrelated. The outputs of the integrate-and-dump circuits update at a relatively slow rate (in kHz) compared to the 160 MHz clock frequency of the system. Therefore, software registers in the ARM core in the Xilinx Virtex-6 FPGA of the ROACH-2 system can be used for update. The software registers are read into the random access memory of the host computer using a Python script. Due to the limited space, the experimental verification of the

2-D FFT-based spectral measurements is reserved for as future work.

D. Experimental Setup

The experimental setup is shown in Fig. 4(a), and the measurements are carried out with the antenna array placed in two different situations as shown in Fig. 6(a). For each beam output corresponding to a spatial-FFT bin, the energy detector is configured to integrate $160,000$ temporal samples, corresponded to 1 ms of time duration. The system is configured to produce 1000 samples of such outputs, corresponded to 1 s of time duration.

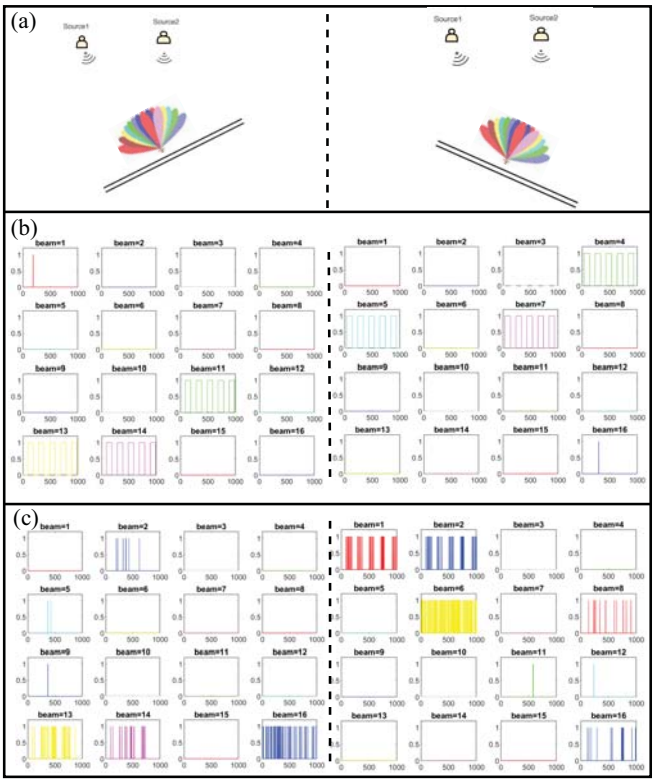

X-axis: time(ms), Y-axis:Spectral Occupancy

Fig. 6. (a) Different situations in which measurements are performed; (b) measurements for the case of known RF sources; (c) real-time measurements using Wi-Fi access points. The detected energy is subjected to thresholding to make a binary decision for spectral occupancy.

E. Control Experiments with Known Sources and Directions

As a proof of concept of our directional sensor, we consider directional sensing of known sources with fixed carrier frequencies. To this end, we transmit a RF signal using on-off keying on the signal by a 5 Hz square wave. So, in a 1 s duration, RF signal contain 5 pulses. Fig. 6(b) shows the computed received energy per beam for a transmission frequency of 2.412 GHz (802.11n Wi-Fi channel number 1) while the LO frequency is set to 2.4 GHz. It can be observed that the beams containing energy are shifted according to the array direction verifying the performance of our directional sensor.

F. Real-World Measurements

The experiment described in section V-E is repeated in an indoor environment with the presence of real Wi-Fi access points. The integration is performed for the same time duration of 1 s. The corresponding measurements are shown in Fig. 6(c). For this real-time measurements, the two sources are kept 30° apart. As expected, we observe the bins/beams that contain significant energy is shifted to the bins in one quadrant to the other with corresponding directions where the sources are placed. It is noted that the case we consider here only corresponds to the antenna array placed in the two quadrants, as shown in Fig. 6(a), and is not exactly aligned for the case of known RF transmission and real-world measurements. Hence, this accounts for a mismatch in the results in beam directions in both cases.

VI. Future Work

The directional sensing system will be extended to incorporate higher-order statistical techniques for extracting information and features of RF sources. Our recent progress with modulation recognition using deep learning [36] will be extended to fully-parallelized digital computing architectures. We will consider spectral correlation function and deep belief networks for high-performance inference and will propose novel computational architectures. These will be implemented in the Virtex-6 FPGA in the ROACH-2 system for real-time sensing. Furthermore, signal parameters such as direction, polarization, frequency, bandwidth, SNR, signal to interference ration (SIR), modulation type, doppler signatures, distortion and echoes (multipath effects) and other waveform dependent parameters will be extracted using algorithms based on linear-systems theory and non-linear higher-order statistical methods. More over, we plan to employ machine learning techniques to recognize previously encountered or specific types of electromagnetic environments. These extracted features can be utilized in upper layers of the wireless communication systems for a variety of intelligent applications including localization and tracking of RF sources, RF source identification, and adaptation of cognitive radio networks.

VII. Conclusions

An FFT-based spatio-temporal RF directional sensing system is proposed for the 2.4 GHz ISM band. The system consists of 16-element patch antenna array and a multi-beam beamformer, implemented on the ROACH-2 based FPGA system. The proposed system performs sensing over 16 look directions simultaneously and each beam output is analyzed through a temporal FFT in order to sense spectra of RF signals corresponding to each beams. Experimental measurements obtained for Wi-Fi devices with a single Wi-Fi channel verify the proof-of-concept directional sensing of the proposed system.

Acknowledgment

A. Madanayake and X. Wang are grateful for US National Science Foundation (NSF) awards ECCS 1854798 and ECCS 1731238, respectively.

REFERENCES

[1] J. Mitola and G. Q. Maquire, "Cognitive radio: making software radios more personal," *IEEE Personal Communications*, vol. 6, no. 4, pp. 13–18, 1999.

[2] S. Haykin, "Cognitive radio: Brain-empowered wireless communications," *IEEE Journal on Selected Areas in Communications*, vol. 22, no. 2, pp. 201–220, 2005.

[3] A. Ali and W. Hamouda, "Advances on spectrum sensing for cognitive radio networks: Theory and applications," *IEEE Communications Surveys & Tutorials*, vol. 19, no. 2, pp. 1277–1304, 2017.

[4] C. Wijenayake, A. Madanayake, J. Kota, and L. T. Bruton, "Space-time spectral white spaces in cognitive radio: Theory, algorithms, and circuits," *IEEE Journal on Emerging and Selected Topics in Circuits and Systems*, vol. 3, no. 4, pp. 640–653, 2013.

[5] L. T. Bruton and N. R. Bartley, "Three-Dimensional Image Processing Using the Concept of Network Resonance," *IEEE Transactions on Circuits and Systems*, vol. CAS-32, no. 7, pp. 664–672, Jul. 1985.

[6] D. E. Dudgeon and R. M. Mersereau, *Multidimensional Digital Signal Processing*. Englewood Cliffs, NJ: Prentice-Hall, 1984.

[7] Q. Zhao and B. M. Sadler, "A survey of dynamic spectrum access," *IEEE Signal Processing Magazine*, vol. 24, no. 3, pp. 79–89, 2007.

[8] M. Höyhtyä, A. Mämmelä, M. Eskola, M. Matinmikko, J. Kalliovaara, J. Ojaniemi, J. Suutala, R. Ekman, R. Bacchus, and D. Roberson, "Spectrum occupancy measurements: A survey and use of interference maps," *IEEE Communications Surveys & Tutorials*, vol. 18, no. 4, pp. 2386–2414, 2016.

[9] X. Wang, J. Liu, W. Chen, and Z. Cao, "CORE-4: Cognition oriented relaying exploiting 4-D spectrum holes," in *Proc. 7th International Wireless Communications and Mobile Computing Conference*, 2011, pp. 1982–1987.

[10] C. Guo, X. Wu, C. Feng, and Z. Zeng, "Spectrum sensing for cognitive radios based on directional statistics of polarization vectors," *IEEE Journal on Selected Areas in Communications*, vol. 31, no. 3, pp. 379–393, 2013.

[11] C. Lee and M. Haenggi, "Delay analysis of spatio-temporal channel access for cognitive networks," in *Proc. IEEE International Conference on Communications*, 2011, pp. 1–5.

[12] C. Liu and M. Jin, "Maximum-minimum spatial spectrum detection for cognitive radio using parasitic antenna arrays," in *Proc. IEEE/CIC International Conference on Communications in China (ICCC)*, 2014, pp. 365–369.

[13] W. Na, J. Yoon, S. Cho, D. Griffith, and N. Golmie, "Centralized cooperative directional spectrum sensing for cognitive radio networks," *IEEE Transactions on Mobile Computing*, vol. 17, no. 6, pp. 1260–1274, 2018.

[14] R. Qian, M. Sellathurai, and T. Ratnarajah, "Directional spectrum sensing for cognitive radio using ESPAR arrays with a single RF chain," in *Proc. European Conference on Networks and Communications (EuCNC)*, 2014, pp. 1–5.

[15] D. Wilcox, E. Tsakalaki, A. Kortun, T. Ratnarajah, C. B. Papadias, and M. Sellathurai, "On spatial domain cognitive radio using single-radio parasitic antenna arrays," *IEEE Journal on Selected Areas in Communications*, vol. 31, no. 3, pp. 571–580, 2013.

[16] B. H. Qureshi, R. K. Sharma, N. Murtaza, M. Grimm, A. Krah, M. A. Hein, A. Heuberger, and R. S. Thoma, "Exploiting spatial dimension in spectrum sensing using a sector antenna: A ray tracer based analysis," in *Proc. IEEE 77th Vehicular Technology Conference (VTC Spring)*, 2013, pp. 1–5.

[17] H. Sarvanko, M. Höyhtyä, M. Matinmikko, and A. Mämmelä, "Exploiting spatial dimension in cognitive radios and networks," in *Proc. 6th International ICST Conference on Cognitive Radio Oriented Wireless Networks and Communications (CROWNCOM)*, 2011, pp. 360–364.

[18] Z. Xu, Q. Liu, C. Zhao, Z. Zhou, and K. S. Kwak, "Spectrum sense utilizing multi-antenna beams scanning in cognitive radio networks," in

[20] G. Zhao, J. Ma, G. Ye Li, T. Wu, Y. Kwon, A. Soong, and C. Yang, "Spatial spectrum holes for cognitive radio with relay-assisted direc-

Proc. 9th International Symposium on Communications and Information Technology, 2009, pp. 1369–1374.

[19] H. Yazdani and A. Vosoughi, "On cognitive radio systems with directional antennas and imperfect spectrum sensing," in *Proc. IEEE International Conference on Acoustics, Speech and Signal Processing (ICASSP)*, 2017, pp. 3589–3593.
tional transmission," *IEEE Transactions on Wireless Communications*, vol. 8, no. 10, pp. 5270–5279, 2009.

[21] Y. Yagi, T. Ohno, H. Murata, K. Yamamoto, and S. Yoshida, "Impact of directional antenna of primary system receiver in spectrum sensing: A case study," *IEEE Communications Letters*, vol. 15, no. 3, pp. 308–310, 2011.

[22] M. Rademacher, K. Jonas, and M. Kretschmer, "Quantifying the spectrum occupancy in an outdoor 5 GHz WiFi network with directional antennas," in *Proc. IEEE Wireless Communications and Networking Conference (WCNC)*, 2018, pp. 1–6.

[23] X. Wang, S. Chaudhari, M. Laghate, and D. Cabric, "Wideband spectrum sensing measurement results using tunable front-end and FPGA implementation," in *51st Asilomar Conference on Signals, Systems, and Computers*, 2017, pp. 499–503.

[24] A. Madanayake, C. Wijenayake, N. Tran, T. Cooklev, S. V. Hum, and L. T. Bruton, "Directional spectrum sensing using tunable multi-D space-time discrete filters," in *Proc. IEEE International Symposium on a World of Wireless, Mobile and Multimedia Networks (WoWMoM)*, 2012, pp. 1–6.

[25] A. Madanayake, N. Udayanga, C. Wijenayake, M. Almalkawi, and V. Devabhaktuni, "Directional cyclostationary feature detectors using 2-D IIR RF spiral-antenna beam digital filters," in *Proc. IEEE International Symposium on Circuits and Systems (ISCAS)*, 2014, pp. 2499–2502.

[26] S. Haykin, *Array Signal Processing*. Englewood Cliffs, NJ: Prentice-Hall, 1985.

[27] T. K. Gunaratne and L. T. Bruton, "Beamforming of broad-band bandpass plane waves using polyphase 2-D FIR trapezoidal filters," *IEEE Transactions on Circuits and Systems I*, vol. 55, no. 3, pp. 838–850, Apr. 2008.

[28] T. K. Gunaratne and L. T. Bruton, "Broadband Beamforming of Bandpass Plane Waves using 2D FIR Trapezoidal Filters at Baseband," in *APCCAS 2006 - 2006 IEEE Asia Pacific Conference on Circuits and Systems*, Dec 2006, pp. 546–549.

[29] R. G. Lyons, *Understanding Digital Signal Processing*, 3rd ed. Upper Saddle River, NJ: Prentice Hall, 2011.

[30] K. W. Martin, "Complex signal processing is not complex," *IEEE Transactions on Circuits and Systems I*, vol. 51, no. 9, pp. 1823–1836, Sep. 2004.

[31] V. Ariyarathne, V. A. Coutinho, S. Pulipati, A. Madanayake, R. T. Wijesekara, C. U. S. Edussooriya, L. T. Bruton, T. K. Gunaratne, and R. J. Cintra, "Real-time 2-D FIR trapezoidal digital filters for 2.4 GHz aperture receiver applications," in *Moratuwa Engineering Research Conference*, 2018, pp. 1–6.

[32] S. Pulipati, V. Ariyarathna, A. Madanayake, R. T. Wijesekara, C. U. S. Edussooriya, and L. T. Bruton, "A 16-element 2.4-GHz multi-beam array receiver using 2-D spatially-bandpass digital filters," *IEEE Transactions on Aerospace and Electronic Systems*, pp. 1–10, 2019, accepted.

[33] R. E. Blahut, *Fast Algorithms for Signal Processing*. Cambridge University Press, 2010.

[34] V. Ariyarathna, D. F. G. Coelho, S. Pulipati, R. J. Cintra, F. M. Bayer, V. S. Dimitrov, and A. Madanayake, "Multibeam digital array receiver using a 16-point multiplierless DFT approximation," *IEEE Transactions on Antennas and Propagation*, vol. 67, no. 2, pp. 925–933, Feb 2019.

[35] "Reconfigurable open architecture computing hardware (ROACH-2) FPGA platform." [Online]. Available: https://casper.berkeley.edu/wiki/ROACH-2

[36] G. J. Mendis, J. Wei, and A. Madanayake, "Deep learning based radio-signal identification with hardware design," *IEEE Transactions on Aerospace and Electronic Systems*, pp. 1–1, 2019, accepted.